

Perturbation theory of multi-plane lens effects in terms of mass ratios: Approximate expressions of lensed-image positions for two lens planes

Koji IZUMI and Hideki ASADA

Faculty of Science and Technology, Hirosaki University, Hirosaki 036-8561, Japan

Continuing work initiated in an earlier publication (Asada, MNRAS **394**, (2009) 818), we make a systematic attempt to determine, as a function of lens and source parameters, the positions of images by multi-plane gravitational lenses. By extending the previous single-plane work, we present a method of Taylor-series expansion to solve the multi-plane lens equation in terms of mass ratios except for the neighborhood of the caustics. The advantage of this method is that it allows a systematic iterative analysis and clarifies the dependence on lens and source parameters. In concordance with the multi-plane lensed-image counting theorem that the lower bound on the image number is 2^N for N planes with a single point mass on each plane, our iterative results show how 2^N images are realized. Numerical tests are done to investigate if the Taylor expansion method is robust. The method with a small mass ratio works well for changing a plane separation, whereas it breaks down in the inner domain near the caustics.

§1. Introduction

Gravitational lensing has become an important subject in modern astronomy and cosmology.^{1),2)} It has many applications as gravitational telescopes in various fields ranging from extra-solar planets to dark matter and dark energy at cosmological scales.³⁾ For instance, it is successful in detecting extra-solar planetary systems.^{8),7),6),5),4)} Gaudi et al.⁹⁾ have found an analogy of the Sun-Jupiter-Saturn system through lensing. Recently gravitational lensing has been used to constrain modified gravity at cosmological scale.¹⁰⁾

This paper considers the gravitational lensing by point-mass systems on multiple planes, where the number of planes is arbitrary. Such a multi-plane treatment is important. In microlensing studies, we usually assume a binary lens on a single lens plane. In order to discuss its validity, we can consider two lens planes and later take the limit that two lens planes merge. In this way, it will become possible to estimate the effect caused by a separation between the double lens planes. Another importance is for gravitational lensing in cosmology. Clearly, galaxies at different redshifts and dark matter inhomogeneities must be described by not a single-plane but multi-plane method.

It has long been a challenging problem to express the image positions as functions of lens and source parameters.^{11),12)} For this purpose, we present a method of Taylor-series expansion to solve the multi-plane lens equation in terms of mass ratios by extending the previous single-plane work.¹³⁾ In particular, we carefully investigate, as a non-trivial task, the denominators of the lens equation with singular points.

The multi-plane lensed-image counting theorem states that the lower bound on the image number is 2^N for N planes with a single point mass on each plane (page

458 in Petters, Levine and Wambsganss¹⁴⁾ and references therein). However, the counting theorem tells nothing about the image positions. Therefore, it is important to discuss *how* such image positions are realized in an analytical method.

Under three assumptions of weak gravitational fields, thin lenses and small deflection angles, gravitational lensing is usually described as a mapping from the lens plane onto the source plane.⁸⁾ Bourassa and Kantowski^{15),16)} introduced a complex notation to describe gravitational lensing. Their notation was used to describe lenses with elliptical or spheroidal symmetry.^{17),18),19)}

For N point lenses, Witt²⁰⁾ succeeded in recasting the lens equation into a single-complex-variable polynomial. This is in an elegant form and thus has been often used in investigations of point-mass lenses. The single-variable polynomial due to N point lenses on a single plane has the degree of $N^2 + 1$, though the maximum number of images is known as $5(N-1)$.^{23),24),21),22)} This means that unphysical roots are included in the polynomial (for detailed discussions on the disappearance and appearance of images near fold and cusp caustics for general lens systems, see also Petters, Levine and Wambsganss¹⁴⁾ and references therein). Following Asada,¹³⁾ we consider the lens equation in dual complex variables, so that we can avoid inclusions of unphysical roots.

This paper is organized as follows. In Section 2, the formulation of multi-plane lens systems with complex variables is briefly summarized. The lens equation is iteratively solved. In section 3, we present iterative solutions for a two-plane case and give an algorithm for computing image positions for an arbitrary number of lens planes in terms of mass ratios. In section 4, we discuss how lensed-image positions are realized in the present method. Section 5 presents numerical tests. Section 6 is devoted to the conclusion.

§2. Basic Formulation

2.1. Multi-plane lens equation

We consider lens effects by N point masses, each of which is located at different angular diameter distances D_i ($i = 1, 2, \dots, N$) from the observer, where $D_1 \leq D_2 \leq \dots \leq D_N$. For this case, we prepare N lens planes and assume the thin-lens approximation for each lens plane.^{25),26)}

All the deflectors line up in small angles and all are far away from caustics. Note that the above lensing setup is idealized. In the real universe, it is rare to find a single isolated lensing mass on each plane. We consider that contributions from masses at large angles are taken into account in the definition of the angular distance on average.^{27),28)} In other words, we focus on effects by a local mass distribution along the line of sight.

First of all, angular variables are normalized in the unit of the angular radius of the Einstein ring as

$$\theta_E = \sqrt{\frac{4GM_{tot}D_{1S}}{c^2D_1D_S}}, \quad (2.1)$$

where we put the total mass on the first plane at D_1 , G denotes the gravitational

constant, c means the light speed, M_{tot} is defined as the total mass $\sum_{i=1}^N M_i$ and D_1 , D_S and D_{1S} denote angular diameter distances between the observer and the first mass, between the observer and the source, and between the first mass and the source, respectively.

Recursively one can write down the multi-plane lens equation.^{25),27)} In the vectorial notation, the two-plane lens equation is written as

$$\beta = \theta - \left(\nu_1 \frac{\theta - \ell_1}{|\theta - \ell_1|^2} + \nu_2 d_2 \frac{\theta - \nu_1 \delta_2 \frac{\theta - \ell_1}{|\theta - \ell_1|^2} - \ell_2}{|\theta - \nu_1 \delta_2 \frac{\theta - \ell_1}{|\theta - \ell_1|^2} - \ell_2|^2} \right), \quad (2.2)$$

where β , θ , ℓ_1 and ℓ_2 denote the positions of the source, image, first and second lens objects, respectively. Here, ν_i denotes the mass ratio of each lens object as $\nu_i \equiv M_i M_{tot}^{-1}$, and we define d_2 and δ_2 as

$$d_2 \equiv \frac{D_1 D_{2s}}{D_2 D_{1s}}, \quad (2.3)$$

$$\delta_2 \equiv \frac{D_S D_{12}}{D_2 D_{1S}}. \quad (2.4)$$

It is convenient to use complex variables when algebraic manipulations are done. In a formalism based on complex variables, two-dimensional vectors for the source, image and lens positions are denoted as $w = \beta_x + i\beta_y$, $z = \theta_x + i\theta_y$, and $\epsilon_i = \ell_{ix} + i\ell_{iy}$, respectively. Figure 1 shows our notation for the multi-plane lens system. Here, z is on the complex plane corresponding to the first lens object that finally deflects light rays and thus z means the direction of a lensed image.

By employing the complex formalism, the two-plane lens equation is rewritten as

$$w = z - \left(\frac{1 - \nu}{z^*} + \frac{\nu d_2}{z^* - \epsilon^* - \frac{(1 - \nu)\delta_2}{z}} \right), \quad (2.5)$$

where the asterisk $*$ means the complex conjugate and we use the identity as $\nu_1 + \nu_2 = 1$ to delete ν_1 and ν denotes ν_2 . Note that we choose the center of the complex coordinate as the first mass position. Then, we have $\epsilon_1 = 0$ and simply denote $\epsilon \equiv \epsilon_2$, which is the projected relative position of the second mass with respect to the first one. The lens equation is non-analytic because it contains not only z but also z^* .

2.2. Iterative solutions

The mass ratio does not exceed the unity by its definition. Therefore, we use a simple method of making expansions in terms of the mass ratios. One can delete ν_1 by noting the identity as $\sum_i \nu_i = 1$.

§3. Image Positions

3.1. Two lens planes

At the zeroth order in ν , the two-plane lens equation becomes simply

$$w = z_{(0)} - \frac{1}{z_{(0)}^*}, \quad (3.1)$$

which is rewritten as

$$z_{(0)}z_{(0)}^* - 1 = wz_{(0)}^*. \quad (3.2)$$

The L.H.S. of the last equation is purely real so that the R.H.S. must be real. Unless $w = 0$, therefore, one can put $z_{(0)} = Aw$ by introducing a certain real number A . By substituting $z_{(0)} = Aw$ into Eq. (3.2), one obtains a quadratic equation for A as

$$ww^*A^2 - ww^*A - 1 = 0. \quad (3.3)$$

This is solved as

$$\begin{aligned} A &= \frac{1}{2} \left(1 \pm \sqrt{1 + \frac{4}{ww^*}} \right) \\ &\equiv A_{\pm}, \end{aligned} \quad (3.4)$$

which gives $z_{(0)}$ as $A_{\pm}w$.

In the particular case of $w = 0$, Eq. (3.2) becomes $|z_{(0)}| = 1$, which is nothing but the Einstein ring. In the following, we assume a general case of $w \neq 0$.

Regarding the denominator of Eq. (2.5), we make an expansion in ν as

$$zz^* - \epsilon^*z - (1 - \nu)\delta_2 \equiv \sum_{p=0}^{\infty} \nu^p f_p, \quad (3.5)$$

where we formally obtain

$$f_0 = z_{(0)}z_{(0)}^* - \epsilon^*z_{(0)} - \delta_2, \quad (3.6)$$

$$f_1 = z_{(0)}z_{(1)}^* + z_{(1)}z_{(0)}^* - \epsilon^*z_{(1)} + \delta_2, \quad (3.7)$$

$$f_2 = z_{(0)}z_{(2)}^* + z_{(1)}z_{(1)}^* + z_{(2)}z_{(0)}^* - \epsilon^*z_{(2)}. \quad (3.8)$$

By choosing $z_{(0)}$ as $A_{\pm}w$, the two-plane lens equation becomes at $O(\nu)$

$$z_{(1)} + az_{(1)}^* = b_1, \quad (3.9)$$

where we define

$$\begin{aligned} a &\equiv \frac{1}{(z_{(0)}^*)^2}, \\ b_1 &\equiv - \left(\frac{1}{z_{(0)}^*} - d_2 \frac{z_{(0)}}{f_0} \right). \end{aligned} \quad (3.10)$$

The above equation is linear in $z_{(1)}$ and thus easily solved as

$$z_{(1)} = \frac{b_1 - ab_1^*}{1 - aa^*}. \quad (3.11)$$

Next, we consider the two-plane lens equation at $O(\nu^2)$. It is written as

$$z_{(2)} + az_{(2)}^* = b_2, \quad (3.12)$$

where we define

$$b_2 = az_{(1)}^* + \frac{a(z_{(1)}^*)^2}{z_{(0)}^*} + \frac{d_2}{f_0} \left(z_{(1)} - z_{(0)} \frac{f_1}{f_0} \right). \quad (3.13)$$

This equation is linear in $z_{(2)}$ and thus easily solved as

$$z_{(2)} = \frac{b_2 - ab_2^*}{1 - aa^*}. \quad (3.14)$$

Let us move to $O(\nu^3)$, for which the two-plane lens equation is linearized as

$$z_{(3)} + az_{(3)}^* = b_3, \quad (3.15)$$

where we define

$$b_3 = - \left[a \left\{ a(z_{(1)}^*)^3 - \frac{2z_{(1)}^*z_{(2)}^*}{z_{(0)}^*} - z_{(2)}^* + \frac{(z_{(1)}^*)^2}{z_{(0)}^*} \right\} - \frac{d_2}{f_0} \left\{ z_{(2)} - z_{(1)} \frac{f_1}{f_0} + z_{(0)} \left(-\frac{f_2}{f_0} + \frac{f_1^2}{f_0^2} \right) \right\} \right]. \quad (3.16)$$

This equation is easily solved as

$$z_{(3)} = \frac{b_3 - ab_3^*}{1 - aa^*}. \quad (3.17)$$

In the above, we have considered a rather general case that the last term in the two-plane lens equation (2.5) is not divergent. Let us investigate the remaining case that the denominator of the last term vanishes, which is expressed as

$$zz^* - (1 - \nu)\delta_2 = \epsilon^*z. \quad (3.18)$$

The left hand side is real and hence the right hand side must be real. Therefore, substituting $z = k\epsilon$ for a real number k into the above equation leads to a quadratic equation for k as

$$k^2 - k - \frac{(1 - \nu)\delta_2}{\epsilon\epsilon^*} = 0. \quad (3.19)$$

This is solved to obtain $z = z_+$ or $z = z_-$. Here, we define

$$z_+ \equiv \frac{\epsilon + \sqrt{\epsilon^2 + 4\nu_1\delta_2\epsilon(\epsilon^*)^{-1}}}{2}, \quad (3.20)$$

$$z_- \equiv \frac{\epsilon - \sqrt{\epsilon^2 + 4\nu_1\delta_2\epsilon(\epsilon^*)^{-1}}}{2}, \quad (3.21)$$

where they are not expanded in ν as an effective renormalization. The reason for avoiding an expansion in the denominator is as follows. If an expansion in ν were done in the denominator, we would see a third-order pole (or higher one) in the lens equation. This would lead to more complicated iterations. In order to avoid it, therefore, we do not expand the denominator. We exactly treat it.

It should be noted that the zeros of the denominator are the positions of the lens objects in a single-plane lens equation,¹³⁾ whereas the zeros for the present case are not the lens positions but located near the lens positions with a certain correction due to a separation between the planes.

We consider the particular case as $z_{(0)} = z_{\pm}$. Then, regarding the denominator of Eq. (2.5), we make an expansion around z_{\pm} in ν as

$$zz^* - \epsilon^*z - (1 - \nu)\delta_2 \equiv \sum_{p=0}^{\infty} \nu^p g_p, \quad (3.22)$$

where we formally obtain

$$\begin{aligned} g_0 &= z_{\pm}z_{\pm}^* - \epsilon^*z_{\pm} - (1 - \nu)\delta_2 \\ &= 0, \end{aligned} \quad (3.23)$$

$$g_1 = z_{\pm}z_{(1)}^* + z_{(1)}z_{\pm}^* - \epsilon^*z_{(1)}, \quad (3.24)$$

$$g_2 = z_{\pm}z_{(2)}^* + z_{(1)}z_{(1)}^* + z_{(2)}z_{\pm}^* - \epsilon^*z_{(2)}. \quad (3.25)$$

Here, g_p is linear in z_p and z_p^* ($p = 1, 2, \dots$). Note that a ν -term appears in Eq. (3.23), because the denominator is exactly treated as a quadratic function.

At the lowest order in ν , the lens equation becomes simply

$$w = z_{\pm} - \frac{1}{z_{\pm}^*} - \frac{d_2}{g_1}. \quad (3.26)$$

This takes the form of $z_{(1)} + a_{\pm}z_{(1)}^* = b_{\pm 1}$ and immediately gives the solution as

$$z_{\pm(1)} = \frac{b_{\pm 1} - a_{\pm}b_{\pm 1}^*}{1 - a_{\pm}a_{\pm}^*}, \quad (3.27)$$

where we define

$$a_{\pm} = \frac{z_{\pm}}{z_{\pm}^* - \epsilon^*}, \quad (3.28)$$

$$b_{\pm 1} = -\frac{d_2 z_{\pm}}{(z_{\pm}^* - \epsilon^*)(w - z_{\pm} + \frac{1}{z_{\pm}^*})}. \quad (3.29)$$

At the next order, the lens equation in the complex-conjugated form is written as

$$0 = z_{\pm(1)} + a_{\pm}z_{\pm(1)}^* + \frac{1}{z_{\pm}^*} - \frac{d_2}{g_1} \left(z_{\pm(1)} - z_{\pm} \frac{g_2}{g_1} \right), \quad (3.30)$$

which is solved as

$$z_{\pm(2)} = \frac{b_{\pm 2} - a_{\pm} b_{\pm 2}^*}{1 - a_{\pm} a_{\pm}^*}. \quad (3.31)$$

Here, we define

$$b_{\pm 2} = -\frac{1}{z_{\pm}^* - \epsilon^*} \times \left((g_1)^2 \frac{z_{\pm(1)} + a z_{\pm(1)}^* + \frac{1}{z_{\pm}^*} - \frac{d_2 z_{\pm(1)}}{g_1}}{d_2 z_{\pm}} + z_{\pm(1)} z_{\pm(1)}^* \right). \quad (3.32)$$

Similarly, we find $z_{(3)}$.

Table I shows a numerical example of image positions obtained iteratively and their convergence.

$z_{(1)}$ tells us an order-of-magnitude estimate of the effect by a separation between the two lens planes. Such a depth effect is characterized by δ_2 , which enters the iterative expressions through z_+ and z_- .

3.2. Three (or more) planes

The above procedure for two lens planes does not seem to work for an arbitrary number of planes, because fifth-order (or higher order) polynomials cannot be solved algebraically as shown by Galois.²⁹⁾

By iterative procedures, however, one can construct roots that are nothing but image positions, because we have expansion parameters. Let us explain this iterative calculation for three-plane lenses as a simple example. One can write down the three-plane lens equation.

First, we neglect ν_3 terms, so that the three-plane lens equation can be reduced to the two-plane one. We have already known how to construct four functions denoting image positions for the two-plane lens equation. Next, in the similar manner to the two-plane case, one can substitute the perturbative image positions into the three-plane lens equation. Four positions with the correction at $O(\nu_3)$ are thus obtained. By using these four linear-order roots, one can find four image positions at $O(\nu_3^2)$. In this way, one can recursively obtain higher order roots.

Other image positions come from the denominator of the last term of the three-plane lens equation. The denominator takes the same form as the two-plane lens equation but with different coefficients (obtained by a replacement as $S \rightarrow 3$ in the subscripts). Hence one can perturbatively construct four other roots. By using these four roots as *seeds* for further iterations, one can construct four roots that can perturbatively satisfy the three-plane lens equation.

Therefore, one can perturbatively construct totally $4 + 4 = 8$ image positions. Clearly this procedure can be used also for four-plane lens systems.

First, we ignore ν_4 terms in the four-plane lens equation, so that the equation can be reduced to the three-plane lens equation. For $N = 3$, one can find eight

image positions as discussed above. Hence, one can iteratively obtain an iterative expression of eight image positions in terms of ν_4 . Next, let us take a look at the denominator of the ν_4 term in the four-plane lens equation. Finding roots of the denominator is essentially similar to that of the three-plane lens equation. This can be done. More eight roots are thus obtained as *seeds* for iterative calculations. One can perturbatively construct totally $8 + 8 = 16$ image positions as functions of the source and lens parameters.

We continue the iterative procedure for five (or more) lens planes *step by step*, so that image positions can be perturbatively obtained as functions of the source and lenses.

Note that two images can merge in the vicinity of the caustics. In this paper, we consider only the regular regions, where images cannot merge. Therefore, zeros of the denominator of the lens equation are not degenerate but distinct.

Table I. Example of image positions by the two-plane lens. We choose $\nu_1 = 9/10$, $\nu_2 = 1/10$, $\epsilon = 3/2$, $w = 2$, $D_1/D_S = 2/5$, $D_2/D_S = 3/5$. Iterative results (denoted as ‘0th’, ‘1st’, ‘2nd’ and ‘3rd’) show a good convergence for the value (denoted as ‘Num’) that is obtained by numerically solving the lens equation. For the same parameter value, a simple ray-tracing method gives numerical values (in the row denoted as ‘Ray’).

Images	1	2	3	4
0th.	2.414213	-0.414213	1.780776	-0.280776
1st.	2.434312	-0.390217	1.731605	-0.276050
2nd.	2.430981	-0.388713	1.732327	-0.275043
3rd.	2.431474	-0.388781	1.732190	-0.274861
Num	2.431396	-0.388766	1.73220	-0.274833
Ray	2.432	-0.393	1.732	-0.279

§4. Realizing Images for N Point Masses

Instead of seeking explicit expressions of image positions, in this section, we discuss how to perturbatively realize lensed-image positions for arbitrary N planes. A hint has appeared in the previous section.

For $N = 2$, the number of the images that are obtained perturbatively is four, which equals to 2^N for $N = 2$. By induction, we shall show how at least 2^N images are realized for N lens planes except for the neighborhood of the caustics.

Let us assume that at least 2^p images are realized for $N = p$. Note that they are not degenerate, since we do not consider the neighborhood of the caustics. What we have to do is to show that at least 2^{p+1} images are realized for $N = p + 1$.

We consider $p + 1$ lens planes. First, let us ignore the $(p + 1)$ -th mass term in the lens equation, so that the equation has the same structure as that for $N = p$. By the assumption for $N = p$, therefore, the reduced equation with neglecting the $(p + 1)$ -th mass term has at least 2^p roots.

Next, the $(p+1)$ -th mass can be considered a new perturber. In the lens equation, the denominator of the fraction with ν_{p+1} has 2^p zeros. Note that it cannot be factored because it is a polynomial mixed with z and z^* . These zeroth-order roots

as *seeds* lead to iterative image positions with the same number.

In total, *at least* $2^p + 2^p = 2^{p+1}$ roots are realized, since our iteration method does not exclude additional solutions. By induction, we understand how at least 2^N images are realized for the multi-plane lens equation for arbitrary N except for the neighborhood of the caustics.

The above method of constructing the image positions means that the image number inequality $\geq 2^N$ is sharp and the lower bound is actually attained. Obstruction points at which the backward-traced light ray hits a lens object and hence does not reach the source plane¹⁴⁾ play a role in the realization in the sense that some of the images are found by investigating the neighborhood of obstruction points.

Before closing this section, we make two remarks. The first remark is made upon a comparison with numerical methods.³⁰⁾ The present method gives analytical expressions of image positions (not their value but their functional forms), so that there can be two merits: 1) Calculations are faster when we obtain the numerical image position. 2) Dependence on the parameters can be made clearer. However, it has a disadvantage, because the result seems to take very lengthy expressions. The second remark is made on multiple roots. The Taylor method assumes that the Taylor series converges, whereas at multiple roots (i.e. merging images) it becomes divergent. Therefore, it is unlikely that the Taylor method can fix the problem when images merge. See also the next section.

§5. Numerical tests

We perform simple ray-tracing calculations in order to investigate if the Taylor expansion method is robust. Table I shows that numerical results by both methods of the Taylor expansion and the ray tracing are in agreement. Note that especially the image No. 1 and 3 are in good agreement, though the image No. 2 and 4 have a few percent difference. This is because light rays corresponding to images No. 2 and 4 pass closer to the primary lens compared with No. 1 and 3 and therefore numerical errors become relatively large.

We make also numerical tests for various values of the lensing parameters in order to investigate the typical size of the cross section, plane separation and mass ratio for which the Taylor expansion breaks down. Figure 2 shows the accuracy when the lensing parameters are numerically changed. Here the relative error for each image for the chosen parameters is denoted as

$$\Delta \equiv \left| \frac{z_{Taylor} - z_{Num}}{z_{Num}} \right|, \quad (5.1)$$

where z_{Taylor} denotes a root obtained by the Taylor expansion method (including the third order corrections) and z_{Num} denotes the root that is obtained by numerically solving the lens equation. Δ_{Max} denotes the largest error among four image positions (for two planes) for the chosen parameter values. For Figure 2, we assume the parameter values that are the same as those in Table I, namely $D_1 = 0.4$, $D_2 = 0.6$ ($D_{12} = 0.2$), $\nu = 0.1$ (mass ratio), $\epsilon = 1.5$ (secondary mass position), $w = 2$ (source position). The Taylor expansion method is robust for a wide range of the parameters

as shown by Figure 2. However, it does not work well in some cases, for instance when a mass ratio is large (i.e. comparable masses), or the source is located in the inner region near the caustics.

In order to quantify the breakdown of the present method, we choose the threshold for Δ_{Max} as 0.01 (one percent). The typical size of the cross section for which the Taylor expansion method breaks down is approximately $\pi \times 0.2^2 \sim 0.1$ (near the primary mass direction) and $\pi \times 1^2 \sim 3$ (around the secondary one), respectively. If the threshold is less than one percent, the two cross sections are merged as a single one. Note that the angle is normalized by the Einstein radius with the total mass located at D_1 . The typical size of the mass ratio to invalidate the Taylor expansion is 0.3. As for the plane separation, the Taylor expansion method seems robust.

§6. Conclusion

We made a systematic attempt to determine, as a function of lens and source parameters, the positions of images by multi-plane gravitational lenses. We presented a method of Taylor-series expansion to solve the multi-plane lens equation in terms of mass ratios except for the neighborhood of the caustics.

In concordance with the multi-plane lensed-image counting theorem that the lower bound on the image number is 2^N for N planes with a single point mass on each plane, our iterative results directly show how 2^N images are realized except for the neighborhood of the caustics.

It is left as a future work to compare the present result with state-of-art numerical simulations.

Acknowledgments

The authors would like to thank M. Kasai and R. Takahashi for stimulating conversations. This work was supported in part (H.A.) by a Japanese Grant-in-Aid for Scientific Research from the Ministry of Education, No. 19035002.

References

- 1) P. Schneider, *Extragalactic Astronomy And Cosmology: An Introduction*, pp. 329-330, (Heidelberg, Springer-Verlag, 2006).
- 2) S. Weinberg, *Cosmology*, pp. 433-468, (Oxford, Oxford Univ. Press, 2008).
- 3) A. Refregier, *Ann. Rev. Astron. Astrophys.* **41** (2003), 645.
- 4) J. P. Beaulieu et al., *Nature* **439** (2006), 437.
- 5) I. A. Bond et al., *Astrophys. J.* **606** (2004), L155.
- 6) A. Gould, A. Loeb, *Astrophys. J.* **396** (1992), 104.
- 7) S. Mao, B. Paczynski, *Astrophys. J.* **374** (1991), 37L.
- 8) P. Schneider, A. Weiss, *Astron. Astrophys.* **164** (1986), 237.
- 9) B. S. Gaudi et al., *Science* **319** (2008), 927.
- 10) R. Reyes et al., *Nature* **464** (2010), 256.
- 11) H. Asada, *Astron. Astrophys.* **390** (2002), L11.
- 12) H. Asada, T. Hamana, M. Kasai, *Astron. Astrophys.* **397** (2003), 825.
- 13) H. Asada, *Mon. Not. R. Astron. Soc.* **394** (2009), 818.
- 14) A. O. Petters, H. Levine, J. Wambsganss, *Singularity theory and gravitational lensing*, pp. 445-465, (Boston, Birkhäuser, 2001).

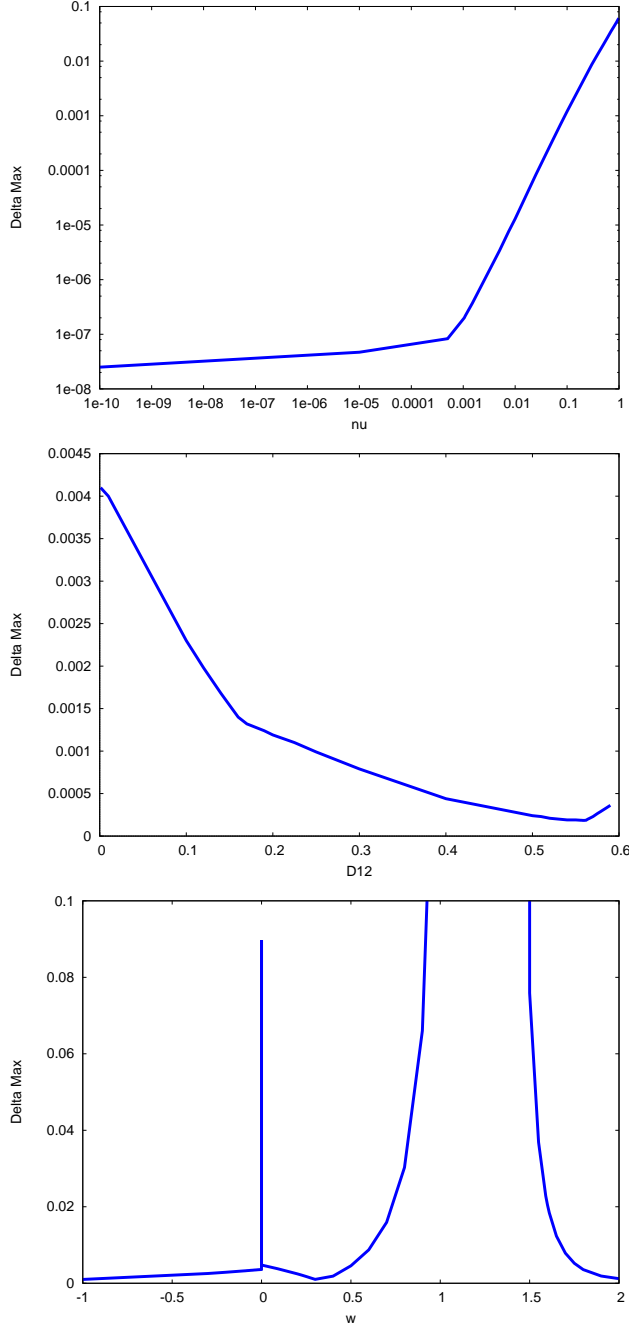


Fig. 2. Numerical tests of the accuracy of the Taylor expansion method with different parameter values. As a reference model for comparisons, we choose the model parameters as $\nu_1 = 9/10$, $\nu_2 = 1/10$, $\epsilon = 3/2$, $w = 2$, $D_1/D_S = 2/5$, $D_2/D_S = 3/5$, which are the same as those in Table 1. Top: Mass ratio as $\nu \equiv \nu_2$ is changed. Middle: Plane separation as D_{12} is changed. Note that $D_{12} < 0.6$ since $D_1 = 0.4$ (normalized by D_S). Bottom: Source position w is changed along the real axis. In actual calculations, smaller parameter steps are adopted to investigate the regions near the primary and secondary caustics. The vertical axis denotes the largest relative error Δ_{Max} of the four images.

- 15) R. R. Bourassa, R. Kantowski, T. D. Norton, *Astrophys. J.* **185** (1973), 747.
- 16) Bourassa R. R., Kantowski R., *Astrophys. J.* **195** (1975), 13.
- 17) U. Borgeest, *Astron. Astrophys.* **128** (1983), 162.
- 18) I. Bray, *Mon. Not. R. Astron. Soc.* **208** (1984), 511.
- 19) T. Schramm, *Astron. Astrophys.* **231** (1990), 19.
- 20) H. J. Witt, *Astron. Astrophys.* **236** (1990), 311.
- 21) D. Khavinson, G. Neumann, *Proc. Amer. Math. Soc.* **134** (2006), 1077.
- 22) D. Khavinson, G. Neumann, *Not. Amer. Math. Soc.* **55** (2008), 666.
- 23) S. H. Rhie, arXiv:astro-ph/0103463 (2001).
- 24) S. H. Rhie, arXiv:astro-ph/0305166 (2003).
- 25) R. Blandford, R. Narayan, *Astrophys. J.* **310** (1986), 568.
- 26) H. Yoshida, K. Nakamura, M. Omote, *Mon. Not. R. Astron. Soc.* **358** (2005), 39.
- 27) P. Schneider, J. Ehlers, E. E. Falco, *Gravitational Lenses*, pp. 25-28, (Heidelberg, Springer-Verlag, 1992).
- 28) K. Tomita, H. Asada, T. Hamana, *Prog. Theor. Phys. Suppl.* **133** (1999), 155.
- 29) B. L. van der Waerden, *Algebra I*, pp. 165-204, (Heidelberg, Springer-Verlag, 1966).
- 30) S. Hilbert, J. Hartlap, S. D. M. White, P. Schneider, *Astron. Astrophys.* **499** (2009), 31.